

## **Part II**

**Desorption**



Trace Surface Analysis Using Ion and Photon Desorption with Resonance Ionization Detection\*

M. J. Pellin, C.E. Young, W.F. Calaway, K. R. Lykke, P. Wurz, and D.M. Gruen  
Argonne National Laboratory, Argonne, IL USA

D. R. Spiegel, A. M. Davis, and R. N. Clayton  
Enrico Fermi Institute, University of Chicago, Chicago, IL 60637, USA

ABSTRACT

Surface Analysis by Resonant Ionization of Sputtered Atoms (SARISA) has demonstrated the ability to detect trace elements at concentrations below 100 ppt. Use of energetic primary ions to desorb surface species is uniquely suited for elemental surface analysis because the ratio between the number of incident energetic ions and the number of ejected surface atoms is easily quantifiable (Sputter Yield). Molecular surface analysis by ion desorption does not possess this advantage, however. In this case, laser desorption followed by resonant or near resonant ionization is often a better analysis tool. Here, the power of resonant ionization detection of desorbed species is demonstrated on hibonite samples (for elemental analysis) and on fullerene samples (for molecular analysis).

INTRODUCTION

Ultrasensitive, *surface* analysis is difficult both because of the few analyte atoms or molecules available and because of interference from the vast excess of bulk material. Surface Analysis by Resonant Ionization of Sputtered Atoms (SARISA) has demonstrated the ability to detect trace elements at concentrations below 100 ppt.<sup>1-5</sup> While the detectable concentration levels are impressive, recent results show that the strength of the SARISA technique may be found in analysis of naturally occurring samples with their wide complement of minor and trace elements. Analysis of such samples is often complicated by several factors including sample charging due to poor sample conductivity, isobaric interferences, and lateral inhomogeneities. Here we will focus on the measurement of Ti in a naturally occurring oxide material (e.g., hibonite). These results demonstrate the ability of SARISA to measure insulating samples without reduction in the Ti useful yield when compared to that of Ti metal.

The development of a straightforward method for the synthesis of macroscopic quantities<sup>6,7</sup> of the truncated icosahedron called Buckminsterfullerene<sup>8</sup>, C<sub>60</sub>, along with other stable closed shell clusters (e.g., C<sub>70</sub> and C<sub>84</sub>) has triggered substantial interest in carbon cluster chemistry. Analysis of solid samples of fullerenes is, therefore, interesting. Unfortunately, the relatively large mass of these species makes study by ion induced desorption or sputtering difficult. This report details time-of-flight mass spectrometry using laser desorption followed by laser ionization with a second laser. Of particular interest, is a velocity distribution of C<sub>60</sub> obtained by suitably delaying the desorbing laser with respect to the ionizing laser.

---

\*Work supported by the U.S. Department of Energy, BES-Materials Sciences, under Contract W-31-109-ENG-38.

## EXPERIMENTAL

Experiments involving Ti atoms were carried out in the SARISA time-of-flight instrument which has been described in detail elsewhere<sup>5</sup>. Three tunable wavelengths were generated using XeCl excimer-pumped dye lasers. For Ti, several schemes have been investigated. The most suitable used a triply resonant scheme with  $\omega_1 = 19323 \text{ cm}^{-1}$  ( $a^3F_2 \rightarrow z^3F_2^0$ ) and  $\omega_2 = 18216 \text{ cm}^{-1}$  ( $z^3F_2^0 \rightarrow e^3F_2$ ). The third laser was then used to pump the excited populations into autoionizing resonances above the ionization potential of the Ti atom ( $55010 \text{ cm}^{-1}$ ). These resonances have not been assigned and were found by scanning the third laser color and monitoring the photoion-induced intensity in the presence of the first two lasers. Many resonances were observed; the most intense at  $\omega_3 = 17668 \text{ cm}^{-1}$  was utilized in these studies. Two resonant schemes investigated are shown in Figure 1.

Hibonite is a naturally occurring mineral with the composition of  $\text{CaAl}_{12-2x}\text{Ti}_x\text{Mg}_x\text{O}_{19}$ , where  $x$  is the concentration of Ti which varies depending on the origins of the mineral. The Ti content of the hibonite sample used in these experiments was 1.2 at.% as verified by electron-induced x-ray fluorescence spectroscopy.<sup>9</sup>

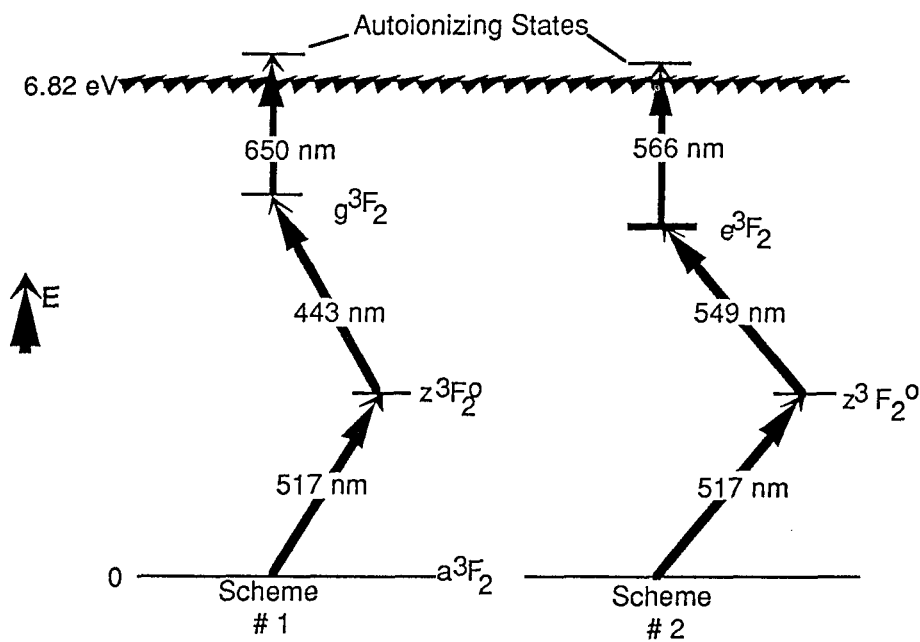


Fig. 1. Two different 3-color resonance ionization schemes which have been used to photoionize Ti.

A Marz-grade Ti metal sample was also mounted in the chamber. The primary ion beam used for these measurements had a diameter of about  $200 \mu\text{m}$ . Samples were prepared by pressing chips of hibonite mineral into a gold foil that was subsequently pressed onto an Al electron microscope stub. The hibonite samples had dimensions between  $90 \mu\text{m}$  and  $300 \mu\text{m}$ .

Fullerene samples were prepared, extracted, and separated using a procedure that has been described elsewhere.<sup>10</sup> Hexane solutions of pure C<sub>60</sub> were allowed to evaporate on a stainless steel sample probe. The films produced in this manner were optically transparent and nonuniform.

For the fullerene measurements, a XeCl excimer laser was used for desorption. A frequency-doubled Coumarin 540A dye laser pumped by a second excimer laser was used for ionization. Both lasers are operated at 1 to 50 Hz repetition rate with laser pulse widths of approximately 20 ns. The wavelengths are 308 nm and 270 nm for desorption and ionization, respectively. The fluence of the desorption laser is held constant at approximately 10-100 mJ/cm<sup>2</sup> for all experiments. The time delay between excimer laser firing times was controlled using a Stanford Instruments DG535 delay generator.

## RESULTS

Figure 2 shows the RIMS spectrum of a small (80 μm x 100 μm) hibonite sample obtained using SARISA IV. The spectrum was obtained from an average of 2000 laser pulses and was obtained with very little sample consumption. Assuming that the sputtering yield (atoms emitted/incident ion) of hibonite is near unity, about 10<sup>7</sup> atoms are sputtered per pulse, i.e.,

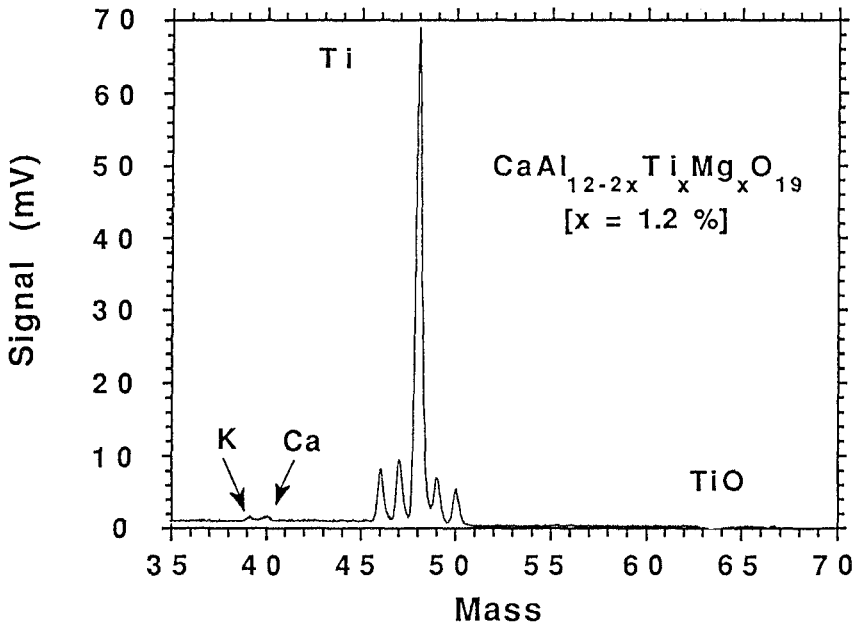


Fig. 2. RIMS spectrum of Ti from a 80 μm x 100 μm hibonite sample.

approximately  $2 \times 10^{10}$  atoms were removed for data acquisition. By analyzing multiple spectra acquired sequentially, we have demonstrated that the Ti isotope ratios can be measured with sub-1% reproducibility on  $\sim 100 \mu\text{m}$  hibonite grains.

A comparison of the Ti signal from a larger ( $250 \mu\text{m} \times 350 \mu\text{m}$ ) sample of hibonite and from pure Ti was made by alternately centering the Ti metal and then the hibonite sample under the primary ion beam in the SARISA apparatus. Comparison in signal could then be made without change in the transmission of the instrument. Table 1 lists the relevant information. One key to this measurement is calibrating the gain of the channel plate detection system.<sup>2,3</sup> The sputtering yield of hibonite was taken to be equivalent to that of rutile.<sup>11</sup> Presently, we are measuring precisely the sputtering yield of hibonite. The measurement presented here may be in error by as much as a factor of 2 because of the uncertainty in the sputtering yield.

Table 1. The relative useful yield of Ti from hibonite and from Ti metal.

Material	Signal Level	Detector Gain	Sputtering Yield	[Ti]	Relative Useful Yield
Ti	54.3	1	1.0	1.0	$Y_{\text{Hib}}/Y_{\text{Ti}}=1.0$
Hibonite	45.1	75	0.9	0.012	

In another set of measurements, we determined the velocity distributions for  $\text{C}_{60}$  clusters laser desorbed from a stainless steel substrate by allowing the desorbed neutral molecules to travel a short distance before being ionized and accelerated into the mass spectrometer. Several velocity distribution measurements were taken to insure reproducibility. These velocity distributions are fitted to a Maxwell-Boltzmann distribution giving reasonably good agreement with the measured data. Figure 3 shows a velocity distribution and a best fit with a Maxwell-Boltzmann distribution for each sample. Theoretical calculations are done to gauge the effect of angular and lateral distributions of the desorbed species on the measured velocity distribution for our particular setup. We found that these have only a small effect compared to other uncertainties encountered in the measurement, although there is a systematic underestimation of the temperature of about 50 K. Taking this into account, we obtain average values for the temperatures of  $2300 \pm 200 \text{ K}$  for the  $\text{C}_{60}$  sample.

There are two distinct models that have been proposed to describe laser desorption by UV photons. These are (i) desorption due to excitation of an antibonding state of the parent or a fragment (cracking) and (ii) thermal desorption due to localized heating by the laser beam.<sup>12-14</sup> We conclude that in our experiment laser desorption is a thermal process for three reasons. First, the measured velocity distribution is well fit by a Maxwell-Boltzmann distribution; second, the temperature derived from this fit is comparable to desorption temperatures previously reported for polymers,<sup>13</sup> and finally, we do not observe fragmentation during the desorption process, which might be expected if a bond-breaking mechanism were active. A more complete description of this work may be found elsewhere.<sup>13-15</sup>

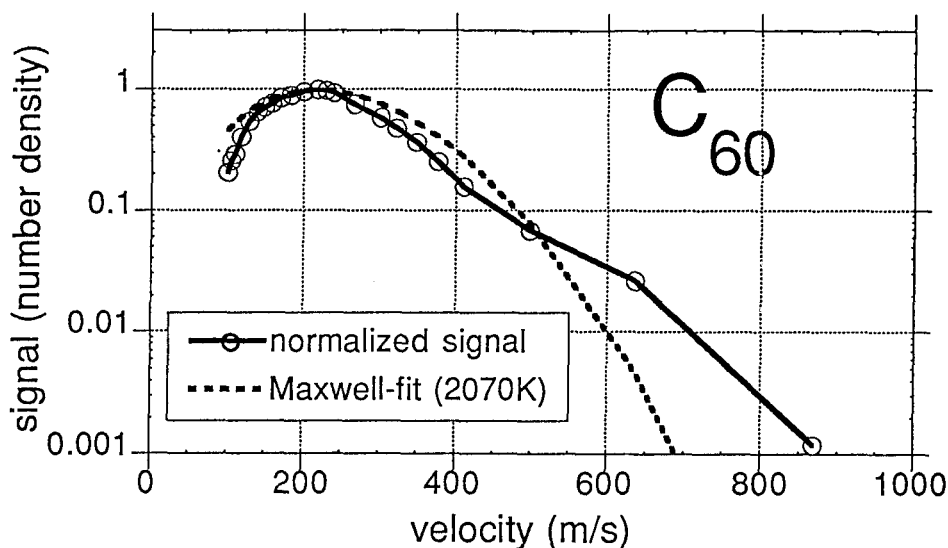


Fig. 3. Velocity distribution for laser desorbed neutral  $C_{60}$ . Dashed curve gives the best fit for a Maxwell-Boltzmann temperature distribution.

#### REFERENCES

- (1) Pappas, D. L.; Hrubowchak, D. M.; Ervin, M. H.; Winograd, N. *Science* **1989**, *243*, 64.
- (2) Blum, J. D.; Pellin, M. J.; Calaway, W. F.; Young, C.E.; Gruen, D. M.; Hutcheon, I. D.; Wasserburg, G. J. *Geochimica* **1990**, *54*, 875 - 881.
- (3) Blum, J. D.; Pellin, M. J.; Calaway, W. F.; Young, C. E.; Gruen, D. M.; Hutcheon, I. D.; Wasserburg, G. J. In *Secondary Ion Mass Spectrometry SIMS VII*; A. Benninghoven, H. W. Huber, and H. W. Werner, Eds.; Wiley: New York, 1990; pp 312-322.
- (4) Blum, J. D.; Pellin, M. J.; Calaway, W. F.; Young, C.E.; Gruen, D. M.; Hutcheon, I. D.; Wasserburg, G. J. *Analytical Chemistry* **1990**, *62*, 209-214.
- (5) Pellin, M. J.; Young, C. E.; Calaway, W. F.; Whitten, J. E.; Gruen, D. M.; Blum, J. D.; Hutcheon, I. D.; Wasserburg, G. J. *Phil. Trans. R. Soc. Lond. A* **1990**, *333*, 133-146.
- (6) Krätschmer, W.; Fostiropoulos, K.; Huffman, D. R. *Chem. Phys. Lett.* **1990**, *170*, 167-170.
- (7) Krätschmer, W.; Lamb, L. D.; Fostiropoulos, K.; Huffman, D. R. *Nature* **1990**, *347*, 354-358.
- (8) Kroto, H. W.; Heath, J. R.; O'Brian, S. C.; Curl, R. F.; Smalley, R. E. *Nature* **1985**, *318*, 162-163.
- (9) Davis, A. *private communication*
- (10) Parker, D. H.; Wurz, P.; Chatterjee, K.; Lykke, K. R.; Hunt, J. E.; Pellin, M. J.; Hemminger, J. C.; Gruen, D. M.; Stock, L. M. *submitted to JACS*.
- (11) Bach, H. *Nucl. Instruments and Methods* **1970**, *84*, 4-12.
- (12) Lazare, S.; Granier, V. *Laser Chem.* **1989**, *89*, 25-40.
- (13) Danielzik, B.; Fabricus, N.; Rowekamp, M.; von der Linde, D. *Appl. Phys. Lett.* **1986**, *48*, 212-214.
- (14) Srinivasan, R.; Braren, B. *Chem. Rev.* **1989**, *89*, 1303-1316.
- (15) Wurz, P.; Lykke, K. R.; Pellin, M. J.; Gruen, D. M. *submitted to Appl. Phys.*